JOURNAL OF GUIDANCE, CONTROL, AND DYNAMICS
Vol. 30, No. 2, March–April 2007

# Control of an Aeroelastic System with Actuator Saturation

Ellen Applebaum* and Joseph Z. Ben-Asher†
*Technion - Israel Institute of Technology, 32000 Haifa, Israel*

DOI: 10.2514/1.20763

**The objective of this study is the semiglobal stabilization of the benchmark active control technology wind-tunnel model developed by NASA Langley Research Center. This study applies established theoretical results to the design of a saturation linear state feedback control law. The framework of this investigation is the construction of the null-controllable region and domains of attraction of the planar antistable subsystem of the higher order model in its canonical modal form. Numerical simulations at different densities of the unstable wind-tunnel system are presented that demonstrate construction and performance of the control law applied to an a priori defined subset of the null-controllable region.**

## Nomenclature

| | | |
|---|---|---|
| $A_{(\cdot)}, B_{(\cdot)}, C_{(\cdot)}$ | = | aeroservoelastic state-space matrices |
| $A(q), B(q), C(q)$ | = | benchmark model state-space matrices |
| $A_1$ | = | planar aeroservoelastic submatrix |
| $A_2$ | = | stable aeroservoelastic submatrix |
| $\boldsymbol{b}$ | = | coefficient input vector of high order system |
| $\boldsymbol{b}_1, \boldsymbol{b}_2$ | = | input coefficient vectors of low-order subsystems |
| $\mathcal{C}$ | = | null-controllable region |
| $\mathcal{C}^a$ | = | asymptotically null-controllable region |
| $\mathcal{C}_1$ | = | null-controllable region of planar system |
| $\overline{C}_1$ | = | closure of the set $C_1$ |
| $\boldsymbol{f}$ | = | gain row vector of $n$th order closed-loop system |
| $\boldsymbol{f}_{\boldsymbol{0}}$ | = | gain row vector of closed-loop planar subsystem |
| $J$ | = | minimum energy quadratic cost function |
| $k, \hat{k}$ | = | gain factors of closed-loop system |
| $n_1$ | = | order of the antistable subsystem |
| $n_2$ | = | order of the stable subsystem |
| $P$ | = | eighth order positive definite solution of algebraic Riccati equation |
| $P1$ | = | $2 \times 2$ positive definite solution of algebraic Riccati equation |
| $P15, P24$ | = | solutions of algebraic Riccati equations for plants #15 and #24 |
| $P_1, P_2, P_3$ | = | submatrices of solution matrix $P$ |
| $Q$ | = | positive definite matrix for Lyapunov equation |
| $q$ | = | air flow dynamic pressure |
| $\mathcal{R}$ | = | reachable region |
| $R^n$ | = | the set of $n$-dimensional real vectors |
| $S$ | = | domain of attraction of closed-loop system |
| $T(\boldsymbol{x}_{a\boldsymbol{0}})$ | = | minimum time for entering planar region |
| $T_M$ | = | maximum time for entering a neighborhood of planar subspace |
| $T_p$ | = | one half period of trajectory along boundary of null-controllable region |
| $t$ | = | time |
| $\mathcal{U}$ | = | set of admissible controls |
| $u$ | = | control deflection command input |
| $\boldsymbol{u}$ | = | vector of admissible control inputs |
| $V(\boldsymbol{x})$ | = | Lyapunov function of state $\boldsymbol{x}$ |
| $v$ | = | control input for time-reversed planar system |
| $\boldsymbol{v}$ | = | vector of admissible control inputs for time-reversed linear system |
| $\boldsymbol{x}$ | = | canonical modal state vector |
| $\boldsymbol{x}^b$ | = | state vector of benchmark wing model |
| $\boldsymbol{x}_a, \boldsymbol{x}_s$ | = | state vectors for antistable and stable canonical matrices |
| $\boldsymbol{x}_{a\boldsymbol{0}}$ | = | initial condition of state trajectory of antistable subsystem |
| $\boldsymbol{x}_{\boldsymbol{0}}^b$ | = | initial state trajectory of benchmark wing model |
| $\boldsymbol{x}_0$ | = | initial condition of state trajectory |
| $y$ | = | output response |
| $\boldsymbol{z}$ | = | state vector time-reversed system |
| $\boldsymbol{z}_a$ | = | state vector time-reversed antistable system |
| $\boldsymbol{z}_f$ | = | reachable state of time-reversed system |
| $z_s^+, z_s^-$ | = | transitional points along extremal trajectory |
| $z_e^+, z_e^-$ | = | equilibrium states for time-reversed linear system with bang–bang control |
| $\alpha$ | = | real part of complex pair |
| $\beta$ | = | imaginary part of complex pair |
| $\gamma, \gamma_1, \gamma_2$ | = | parameters for control construction |
| $\partial(\cdot)$ | = | boundary of regions $C, S$ |
| $\epsilon, \epsilon_0$ | = | parameters in eighth order algebraic Riccati equation |
| $\zeta(P, \rho)$ | = | the level set $\{x \in R^n: x^T P x \leq \rho\}$ |
| $\xi$ | = | $2 \times 1$ vector of elliptic transformation |
| $\rho$ | = | parameter for level surface $x^T P x = \rho$ |
| $\rho_{15}, \rho_{24}$ | = | measured air density for simulated plant models |
| $\phi(t, \boldsymbol{x}_{a\boldsymbol{0}})$ | = | solution trajectory of closed-loop planar subsystem |
| $\psi(t, \boldsymbol{z}_a^{\boldsymbol{0}})$ | = | solution trajectory of closed-loop time-reversed subsystem |
| $\Omega_1, \Omega_2$ | = | parameterized subsets of the null-controllable region |
| $\Omega_1^{\circ}$ | = | interior of set $\Omega_1$ |

*Subscripts*

| | | |
|---|---|---|
| $\boldsymbol{a}$ | = | antistable $2 \times 1$ state vector |
| $a0$ | = | index for initial condition in planar region |
| $e$ | = | index to equilibrium state for bang–bang control $\pm 1$ |
| $f$ | = | index to final system state |
| $M$ | = | index to maximum time $T_M$ |

Received 27 October 2005; revision received 10 March 2006; accepted for publication 27 March 2006. 

*Research Scientist, Faculty of Aerospace Engineering.
†Associate Professor, Faculty of Aerospace Engineering. Associate Fellow AIAA.

| | | |
|---|---|---|
| $p$ | = | index for period of $\partial C$ |
| $\boldsymbol{s}$ | = | stable state vector, extremal trajectory |
| 0 | = | index to parameter$\epsilon$ |
| $\mathbf{0}$ | = | descriptor of gain row vector $\boldsymbol{f}$ |
| 1, 2, 3 | = | indices to submatrices |

*Superscripts*

| | | |
|---|---|---|
| $a$ | = | identifies the asymptotically null-controllable region |
| $b$ | = | identifies benchmark state vector coordinates |
| $m$ | = | $m$-dimensional vector space |
| $n$ | = | $n$-dimensional vector space |
| $n_1$ | = | order of antistable subsystem |
| $n_2$ | = | order of stable subsystem |
| $T$ | = | transpose |

## Introduction

DURING the past several years, flutter suppression techniques have been actively investigated on the benchmark active control technology (BACT) wind-tunnel model developed by NASA Langley Research Center [1–7]. The BACT exhibits classical flutter instability at transonic speeds with system dynamics that vary with the dynamic pressure. The BACT has provided a test bed for the development and testing of passivity-based robust control, linear parameter varying gain scheduling control, $H$-infinity, $\mu$-synthesis generalized predictive control, full order and reduced order linear quadratic Gaussian, and others. The body of flutter suppression techniques developed for the BACT model is based upon a system that can be effectively reduced to a low-order state-space model.

This paper addresses the problem of control saturation in the continuous time linear BACT system. The primary focus is on the theory and techniques that determine domains of attraction of the origin that guarantee stability given control input saturation in a full-state linear feedback system. In this effort, 24 working points of the eighth order BACT model have been considered, each one representing a different dynamic pressure with open-loop dynamics ranging from stable to unstable.

In control law design there are generally two approaches for dealing with actuator saturation. In the first approach, one starts with the control design and then adds problem specific schemes referred to as antiwindup schemes which use ad hoc modifications and require extensive modifications that are validated through numerical simulations. Classical methods of control law design for flutter suppression in the BACT system have tended to use this approach. Optimization methods such as min–max and state-dependent Riccati equation methods have also been applied to flutter suppression with hard constraints on the control input [3,8]. Both methods require validation of controllability and stability for specific initial conditions and control constraints through an iterative process of parameter selection and numerical simulations.

The second approach is the one addressed in this paper: One takes into account the saturation nonlinearity at the outset of the control design in a systematic manner that exploits the entire range of the control surface. There has been considerable research on the problem of stabilization of linear systems subject to control constraints [9–13]. Recently, researchers have laid the theoretical foundation for addressing the stabilization problem in the context of saturated linear feedback [9]. At the heart of the theory is the characterization of the null-controllable region (or, asymptotically null-controllable region), the set of all initial conditions that can be driven to the origin by constrained controls in some finite time (or asymptotically). It has already been established that the asymptotically null-controllable region of an open-loop system that is stabilizable and has all its poles in the closed left-half plane is the entire state space if the constrained control set contains the origin in its interior [14]. The theoretical body of work also addresses the construction of feedback laws that achieve stabilization on the entire or a large portion of the asymptotically null-controllable region. It has recently been shown that feedback laws can be constructed that achieve a domain of attraction large enough to include any a priori given bounded set in the null-controllable region [9]. In particular, Hu and Lin [9] address the construction of feedback laws for stabilization of linear systems with second order antistable subsystems whose complex pair of eigenvalues are located in the closed right-half plane. The BACT model addressed in this study falls into this category. This paper demonstrates the application of previously developed theory to the real-world problem of achieving flutter suppression in an aeroservoelastic system with constrained linear feedback.

## The BACT Model

The BACT system models the vertical linear aeroservoelastic (ASE) dynamic response of a wing section, equipped with an aft flap control surface, suspended in a two-dimensional air flow. The wing has two degrees of freedom: vertical displacement and pitch angle. The flap deflection is actuated via an electrical motor, whose voltage input serves as the system control input. The wing ASE characteristics vary with the air flow dynamic pressure. Figure 1 shows a view of the BACT wind-tunnel model test setup on the pitch and plunge apparatus (PAPA). The BACT wind-tunnel setup consists of a NACA0012 airfoil rectangular wing equipped with an active trailing-edge control surface, two spoilers, and pressure transducers [3].

The BACT model addressed in this study is a single input/single output linear dynamic system, with the following state-space realization:

$$\dot{\boldsymbol{x}}^b = A(q)\boldsymbol{x}^b + B(q)u; \qquad \boldsymbol{x}^b(t=0) = \boldsymbol{x}_{\mathbf{0}}^b \tag{1}$$

$$y = C(q)\boldsymbol{x}^b$$

where the state vector $\boldsymbol{x}^b \in R^8$, $u$ (the control input), and $y$ (the sensor output) $\in R^1$. The first four states represent the wing's vertical displacement and pitch angle ($x_1^b$ and $x_2^b$) and generalized velocities ($x_3^b$ and $x_4^b$). The fifth coordinate ($x_5^b$) models the aerodynamic state. The last three states ($x_6^b$–$x_8^b$) model the third order wing flap electrical actuator dynamics (which is invariant to the air flow dynamic pressure). Accelerometers are the primary sensor outputs for feedback control. In this study, a single accelerometer is located at the wing shear center. The entries of the BACT system matrices $A(q), B(q), C(q)$ were evaluated, using ZAERO software [15,16] for 24 air density discrete values ranging from $5 \times 10^{-5}$ (kgm/m$^3$) to $4 \times 10^{-3}$ (kgm/m$^3$), at a constant air flow velocity of 119 m/s at Mach number 0.77. Dynamic pressures range from 3.8 (N/m$^2$) to 304 (N/m$^2$). For low dynamic pressure values, the system is open-loop stable; it gradually becomes unstable as the dynamic pressure

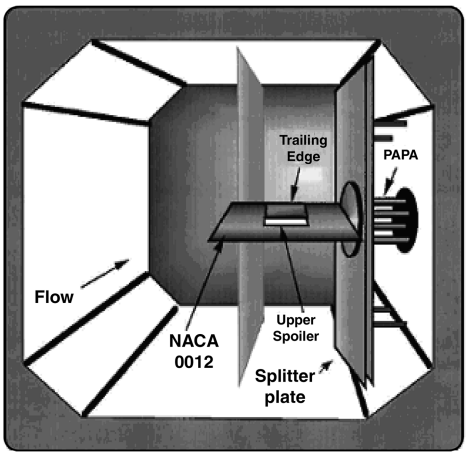


**Fig. 1 BACT wind-tunnel test setup.**

increases. The instability occurs for the first time at a dynamic pressure value of 167.3 ($N/m^2$), corresponding to BACT "plant #15". A conjugate complex pair of poles gradually moves to the right of the complex plane. For all dynamic pressure values, the system is nonminimum phase.

The canonical modal form of the 8th order open-loop BACT model comprises a system submatrix $A_1 \in R^{2\times 2}$ possessing a pair of complex eigenvalues and a *stable* system submatrix $A_2 \in R^{6\times 6}$ whose eigenvalues belong to the open left-hand side complex plane. For BACT plant models #15–#24, the submatrix $A_1$ represents an *antistable* subsystem, whose complex eigenvalues are located in the open right-hand side complex plane. The open-loop BACT system takes the canonical modal form

$$\dot{\boldsymbol{x}} = A\boldsymbol{x} + \boldsymbol{b}u = \begin{bmatrix} A_1 & 0 \\ 0 & A_2 \end{bmatrix} x + \begin{bmatrix} \boldsymbol{b}_1 \\ \boldsymbol{b}_2 \end{bmatrix} u \tag{2}$$

where the respective antistable $(A_1, \boldsymbol{b}_1)$ and stable $(A_2, \boldsymbol{b}_2)$ subsystems are

$$\dot{\boldsymbol{x}}_a = A_1\boldsymbol{x}_a + \boldsymbol{b}_1 u \tag{3}$$

$$\dot{\boldsymbol{x}}_s = A_2\boldsymbol{x}_s + \boldsymbol{b}_2 u \tag{4}$$

The state vector of the antistable subsystem $\boldsymbol{x}_a = \{x_1, x_2\}$ and the state vector of the stable subsystem $\boldsymbol{x}_s = \{x_3, x_4, x_5, x_6, x_7, x_8\}$.

## Building Domains of Attraction: Planar Systems

In the absence of a design specification regarding the size of the domain of attraction it can be shown that any feedback law that stabilizes the linear system (2) without saturation can be made to stabilize the system locally in the presence of actuator saturation. The next section describes the method for obtaining a conservative estimate of such local invariant domains of attraction for the planar antistable subsystem. Following this, the notion of a null-controllable region is introduced along with the method for obtaining domains of attraction for the antistable planar system that are arbitrarily close in size to the null-controllable region. It is shown that a domain of attraction can be constructed containing any a priori bounded subset of the asymptotically null-controllable region. This fact is then used in the construction of an admissible feedback law for stabilization of the higher order BACT model. Next, an algorithm is presented for design and analysis of feedback control laws for continuous time aerodynamic models with actuator saturation that satisfy the theoretical requirements of this study. The final section presents examples of the method for stabilization of the BACT plants #15 and #24.

### Conservative Estimate of Domain of Attraction

For a saturated linear control applied to the antistable subsystem (3), the domain of attraction $S$ of the origin is a subset of the $R^{n_1}$ subspace ($S \subset R^{n_1}$, $n_1 = 2$). For a saturated linear control applied to the stable $n_2$ order subsystem (4), the domain of attraction is the entire $R^{n_2}$ subspace ($n_2 = 6$). A good first step in controller design is to compute a conservative estimate of the domain of attraction for the closed-loop antistable subsystem

$$\dot{\boldsymbol{x}}_a = A_1\boldsymbol{x}_a - \boldsymbol{b}_1 \mathrm{sat}(\boldsymbol{f_0}\boldsymbol{x}_a) \tag{5}$$

where $\boldsymbol{f_0} \in R^{1\times 2}$ is the feedback gain and sat: $R \to R$ is the standard saturation function defined as

$$\mathrm{sat}\,(\boldsymbol{f_0}\boldsymbol{x}_a) = \mathrm{sign}(\boldsymbol{f_0}\boldsymbol{x}_a)\min[1, |\boldsymbol{f_0}\boldsymbol{x}_a|]$$

It has been shown that the origin is the unique equilibrium point of Eq. (5) [9,10]. The state feedback law

$$u = -\mathrm{sat}(\boldsymbol{f_0}\boldsymbol{x}_a) \tag{6}$$

is said to be *stabilizing* if the feedback matrix $[A_1 - \boldsymbol{b}_1\boldsymbol{f_0}]$ is asymptotically stable. The open-loop system (3) and the pair $(A_1, \boldsymbol{b}_1)$ are said to be *stabilizable* if such a feedback law exists. The domain of attraction of the origin is defined as

$$S = \left\{\boldsymbol{x}_{a\mathbf{0}} \in R^2 : \lim_{t\to\infty} \phi(t, \boldsymbol{x}_{a\mathbf{0}}) = \mathbf{0}\right\} \tag{7}$$

where $\phi(t, \boldsymbol{x}_{a\mathbf{0}})$ is the unique solution of Eq. (5) for initial condition $\mathbf{x_{a0}}$. The conservative estimate of the domain of attraction under a saturated stabilizing linear feedback law (6) is computed by solving an algebraic Riccati equation (ARE). The following ARE is solved for positive definite $2 \times 2$ matrix $P1$:

$$A_1^T P1 + P1A_1 - P1\boldsymbol{b}_1\boldsymbol{b}_1^T P1 = 0 \tag{8}$$

This ARE is associated with the minimum energy cost function

$$J = \int_0^\infty u^T(t)u(t)\,\mathrm{d}t$$

The minimum energy gain is computed as $\boldsymbol{f_0} = \boldsymbol{b}_1^T P1$. $P1$ satisfies the following Lyapunov inequality for the stable closed-loop system matrix $[A_1 - \boldsymbol{b}_1\boldsymbol{f_0}]$:

$$(A_1 - \boldsymbol{b}_1\boldsymbol{f_0})^T P1 + P1(A_1 - \boldsymbol{b}_1\boldsymbol{f_0}) < 0 \tag{9}$$

A Lyapunov level set is constructed in the following manner:

$$\zeta(P1, \rho) = \left\{\boldsymbol{x}_a \in R^2 : \boldsymbol{x}_a^T P1 \boldsymbol{x}_a \le \rho\right\}$$

where $\rho > 0$ can be chosen such that $\zeta(P1, \rho) \subseteq \{\boldsymbol{x}_a \in R^2 : -1 < \boldsymbol{f_0}\boldsymbol{x}_a < 1\}$. This follows from the fact that the set $\{\boldsymbol{x}_a : |\boldsymbol{f_0}\boldsymbol{x}_a| < 1\}$ is an open subset of $R^2$ containing the origin. The level set $\zeta(P1, \rho)$ is an invariant subset of $S$ because any state trajectory $\boldsymbol{x}(t)$ of (5) with an initial condition $\boldsymbol{x}_{a\mathbf{0}}$ in $\zeta(P1, \rho)$ remains in $\zeta(P1, \rho)$ for all times $t > 0$. The invariant set $\zeta(P1, \rho)$ serves as a conservative estimate of the domain of attraction and can be transformed into an ellipse using the method of quadratic forms [17].

Figure 2 shows the ellipses that were generated from several selections of $\rho$ for the antistable submatrix $A_1$ of BACT plant #24 with

$$A_1 = \begin{bmatrix} 1.5427 & 23.0449 \\ -23.0449 & 1.5427 \end{bmatrix} \tag{10}$$

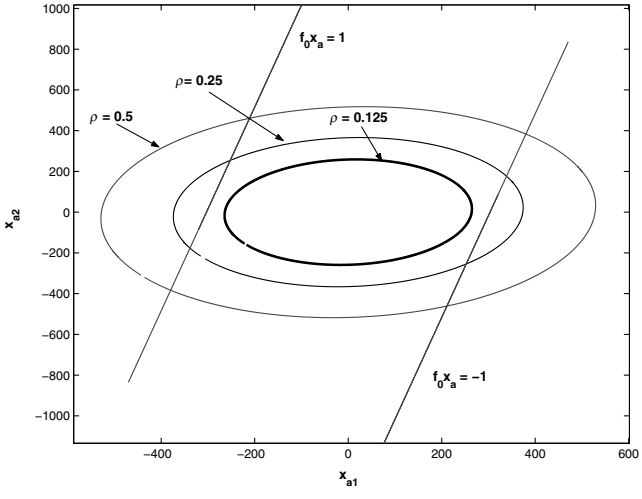


**Fig. 2 Invariant level sets $\zeta(P1, \rho)$ for $\rho = 0.5, 0.25$, and $0.125$.**

$$\boldsymbol{b}_1 = \begin{bmatrix} -1823.519 \\ 239.443 \end{bmatrix} \tag{11}$$

$$\boldsymbol{f_0} = [-0.00033 \quad 0.0007] = \boldsymbol{b}_1^T P1 \tag{12}$$

where $P1$ is the solution of the ARE (8). For $\rho = 0.125$, the level set $\zeta(P1, \rho)$ lies within the interior of the open set $\{\boldsymbol{x}_a: -1 < \boldsymbol{f_0 x}_a < 1\}$.

**Null-Controllable Region**

The concept of a null-controllable region, as introduced in [9], is used to derive a less conservative estimate of the domain of attraction. Consider the general $n$th order linear system

$$\dot{\boldsymbol{x}} = A\boldsymbol{x} + \boldsymbol{bu} \tag{13}$$

where $\boldsymbol{x} \in R^n$ and $\boldsymbol{u} \in R^m$. Let

$$\mathcal{U} = \{\boldsymbol{u}: \boldsymbol{u} \text{ is measurable} \quad \text{and} \quad |\boldsymbol{u}(t)|_\infty = \max_i |u_i(t)| \le 1, \quad \forall\, t \in R\} \tag{14}$$

be the set of admissible controls for Eq. (13).

The null-controllable region $\mathcal{C}$ of system (13) is defined as the set of states for which an admissible control $\boldsymbol{u}$ exists such that the state trajectory $\boldsymbol{x}(t)$ satisfies the criterion that if $\boldsymbol{x}(0) = \boldsymbol{x}_0 \in \mathcal{C}$ then there exists a time $T \in [0, \infty)$ such that $\boldsymbol{x}(T) = 0$. This condition can be rephrased in terms of the reachable region $\mathcal{R}$ for the time-reversed system

$$\dot{\boldsymbol{z}} = -A\boldsymbol{z} - \boldsymbol{bv} \tag{15}$$

The reachable region $\mathcal{R}$ of system (15) consists of all states $\boldsymbol{z}_f$ of state trajectory $\boldsymbol{z}(t)$ that are reachable at some time $T \in [0, \infty)$ for an admissible control $\boldsymbol{v}$ and an initial state $\boldsymbol{z}(0) = 0$. The boundary $\partial\mathcal{C}$ of the null-controllable region $\mathcal{C}$ is identical with the boundary $\partial\mathcal{R}$ of the reachable region $\mathcal{R}$. This follows from the fact that the two systems (13) and (15) have the same curves as trajectories but traverse in opposite directions.

Consider the time-reversed planar subsystem

$$\dot{\boldsymbol{z}}_a = -A_1 \boldsymbol{z}_a - \boldsymbol{b}_1 v \tag{16}$$

where $v \in R^1$ is an admissible control $[|v(t)|_\infty \le 1]$ and the eigenvalues of $A_1$ form a complex pair $(\alpha \pm \beta i), \alpha, \beta > 0$. Denote $\boldsymbol{z}_e^- = A_1^{-1}\boldsymbol{b}_1$ and $\boldsymbol{z}_e^+ = -A_1^{-1}\boldsymbol{b}_1$. The boundary of the reachable region $\partial\mathcal{R}$ is computed as [9]

$$\partial\mathcal{R} = \left\{ \pm (e^{-A_1 t}\boldsymbol{z}_s^- - \int_0^t e^{-A_1(t-\tau)}\boldsymbol{b}_1 \, \mathrm{d}\tau) : t \in [0, T_p) \right\} \tag{17}$$

$$= \left\{ \pm \left[ e^{-A_1 t}\boldsymbol{z}_s^- - (I - e^{-A_1 t})A_1^{-1}\boldsymbol{b}_1 \right] : t \in [0, T_p) \right\} \tag{18}$$

where

$$T_p = \pi/\beta, \qquad \boldsymbol{z}_s^- = \frac{1 + e^{-\alpha T_p}}{1 - e^{-\alpha T_p}} \boldsymbol{z}_e^-$$

Figure 3 illustrates the boundary of the null-controllable region $\partial\mathcal{C}$ in terms of the boundary of the reachable region $\partial\mathcal{R}$ (18) for the antistable planar subsystem of BACT plant #24 (The fixed density $\rho_{24} = 4.0 \times 10^{-3}$). The coordinates of the axes may be expressed in terms of the time-reversed planar subsystem (16) or the planar subsystem (3). As noted in the preceding section, the curves of the antistable system and its time-reversed system are the same. The trajectory along $\partial\mathcal{C}$ goes from $\boldsymbol{z}_s^-$ to $\boldsymbol{z}_s^+$ under the control $v = 1$ and then from $\boldsymbol{z}_s^+$ to $\boldsymbol{z}_s^-$ under the control $v = -1$. The points $\boldsymbol{z}_e^-$ and $\boldsymbol{z}_e^+$ are located in the interior of the null-controllable region for the antistable subsystem consisting of a pair of complex eigenvalues $\alpha \pm \beta = 1.54 \pm 23.0449i$. The extremal trajectory along $\partial\mathcal{C}$ has period $2T_p = 0.26$ s. Notice that this region is significantly larger than the level set $\zeta(P1, \rho = 0.125)$ (Fig. 2).

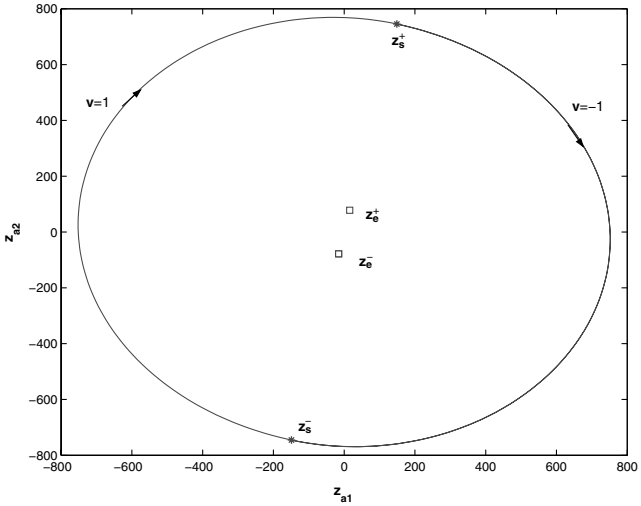


**Fig. 3 Boundary of null-controllable region, plant #24.**

The null-controllable region is used as a basis for extending the domain of attraction of the closed-loop system (5) with saturated linear feedback in the following manner. Consider the closed-loop system

$$\dot{\boldsymbol{x}}_a = A_1 \boldsymbol{x}_a + \boldsymbol{b}_1 u, \; u = -\mathrm{sat}(\boldsymbol{f_0 x}_a) \in \mathcal{U} \tag{19}$$

where $\boldsymbol{f_0} = \boldsymbol{b}_1^T P1$ and $P1$ satisfies the Lyapunov inequality (9). It is shown in [9] that the boundary of $S$ (i.e., $\partial S$) is the unique limit cycle of the planar closed-loop system (19) and the time-reversed system

$$\dot{\boldsymbol{z}}_a = -A_1 \boldsymbol{z}_a + \boldsymbol{b}_1 \, \mathrm{sat}(\boldsymbol{f_0 z}_a) \tag{20}$$

This limit cycle is a stable one for system (20) and an unstable one for (19). Moreover, every trajectory $\psi(t, \boldsymbol{z}_{a\boldsymbol{0}})$, $\boldsymbol{z}_{a\boldsymbol{0}} \neq \boldsymbol{0}$ of (20) converges to the limit cycle. One can therefore determine the boundary of the domain of attraction of the origin by simulating the time-reversed closed-loop system (20). A trajectory $\phi(t, \boldsymbol{x}_{a\boldsymbol{0}})$ of (19) converges to the origin if and only if $\boldsymbol{x}_{a\boldsymbol{0}}$ is inside the limit cycle. Based upon the infinite gain margin property of linear quadratic regulators [18] for $k > 0.5$ the origin is a stable equilibrium of equation

$$\dot{\boldsymbol{x}}_a = A_1 \boldsymbol{x}_a - \boldsymbol{b}_1 \, \mathrm{sat}(k \boldsymbol{f_0 x}_a) \tag{21}$$

The following theorem establishes the semiglobal stabilizability of the planar antistable system with saturation linear feedback and links it to the null-controllable region.

*Theorem 1* [9]: Let $S(k)$ be the domain of attraction of the equilibrium $\boldsymbol{x}_a = 0$ of (21). It can be shown that

$$\lim_{k \to \infty} \mathrm{dist}[S(k), \mathcal{C}] = 0 \tag{22}$$

where $\mathrm{dist}[S(k), \mathcal{C}]$ is the Hausdorff distance between the two sets.

The gain $k$ can be adjusted to produce an arbitrarily large domain of attraction contained in the null-controllable region. Hence, as a consequence of Theorem 1, one can define a priori a bounded subset of the interior of the null-controllable region that lies within the domain of attraction of (21).

Figure 4 shows plots of the boundaries of domains of attraction $S(k)$, $k = 0.51, 0.55, 0.6$ for the closed-loop planar subsystem (21) whose matrices $(A_1, \boldsymbol{b}_1)$ are, respectively, (10) and (11). The dotted line indicates the boundary of the null-controllable region. The minimum energy gain is $\boldsymbol{f_0} = [-0.0033 \quad 0.0007]$. Notice, for increasing values of $k$, the tendency to converge to the null-controllable boundary.

## Stabilization of Higher Order BACT System

This section applies the theory of [9] to establish the semiglobal stabilizability of the higher order open-loop BACT system (2) under

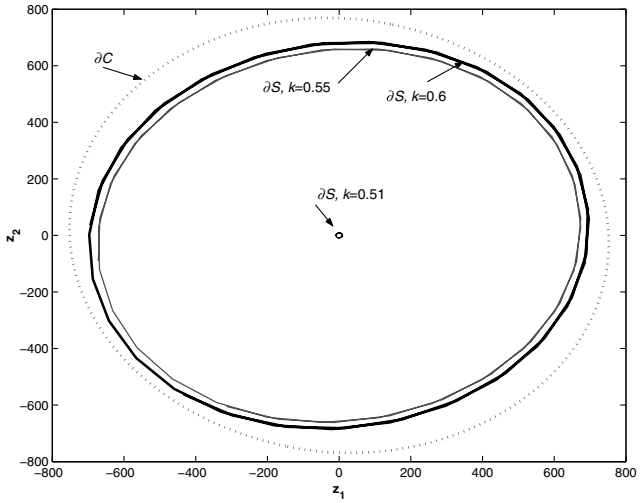


**Fig. 4 Domains of attraction for plant #24 with different $k$ feedbacks.**

saturated control. A bounded subset in the interior of the null-controllable region is defined a priori. A saturation linear state feedback law is designed (assuming the entire state $\boldsymbol{x}$ is measured) such that the bounded subset is contained in the domain of attraction of the origin of the closed-loop system. The following definition forms the basis for characterizing the null-controllable region of the BACT system in terms of its antistable planar subsystem.

A state $\boldsymbol{x}_0$ is said to be asymptotically null-controllable if there exists an admissible control $u$ such that the state trajectory $\boldsymbol{x}(t)$ of system (2) satisfies $\boldsymbol{x}(0) = \boldsymbol{x}_0$ and $\lim_{t\to\infty}\boldsymbol{x}(t) = \boldsymbol{0}$. The set of all states that are asymptotically null-controllable, denoted $\mathcal{C}^a$, is called the asymptotically null-controllable region. The asymptotically null-controllable region of the higher order open-loop BACT system is defined as $\mathcal{C}^a = \mathcal{C}_1 \times R^6$, where $\mathcal{C}_1$ is the null-controllable region of the antistable planar subsystem (3) and the subspace $R^6$ is the null-controllable region of the stable subsystem (4).

The characterization of $\mathcal{C}^a$ for the BACT system can be carried out in terms of $\mathcal{C}_1$. For $\gamma_1 < 1$, define the set

$$\Omega_1(\gamma_1) = \{\gamma_1 \boldsymbol{x}_a \in R^2 : \boldsymbol{x}_a \in \bar{\mathcal{C}}_1\} \subset \mathcal{C}_1 \tag{23}$$

$\Omega_1(\gamma_1)$ lies in the interior of the null-controllable region of the planar antistable subsystem. For $\gamma_2 > 0$, define

$$\Omega_2(\gamma_2) = \{\boldsymbol{x}_s \in R^6 : |\boldsymbol{x}_s| \le \gamma_2\} \tag{24}$$

where $|\cdot|$ is the 2-norm.

Given any $\gamma_1 < 1$ and $\gamma_2 > 0$, a saturated linear state feedback law can be designed such that $\Omega_1(\gamma_1) \times \Omega_2(\gamma_2)$ is contained in the domain of attraction of the equilibrium $\boldsymbol{x} = \boldsymbol{0}$ of the closed-loop BACT system. For a given $\epsilon > 0$ the admissible state feedback law is constructed by solving for a unique positive definite $P(\epsilon)$ the ARE

$$A^T P(\epsilon) + P(\epsilon)A - P(\epsilon)\boldsymbol{b}\boldsymbol{b}^T P(\epsilon) + \epsilon I = 0 \tag{25}$$

By the continuity property of the solution of the Riccati equation [9]

$$\lim_{\epsilon\to 0} P(\epsilon) = \begin{bmatrix} P1 & 0 \\ 0 & 0 \end{bmatrix}$$

where $P1$ is the unique positive definite matrix solution to the ARE (8) associated with the antistable and controllable planar system $(A_1, \boldsymbol{b}_1)$. The gain is defined as $\boldsymbol{f}(\epsilon) = \boldsymbol{b}^T P(\epsilon)$ for the closed-loop BACT system represented as

$$\dot{\boldsymbol{x}} = A - \boldsymbol{b}\ \text{sat}[\boldsymbol{f}(\epsilon)\boldsymbol{x}] \tag{26}$$

A subset of the domain of attraction of the equilibrium $\boldsymbol{x} = \boldsymbol{0}$ of (26) can be constructed using the Lyapunov level set

$$D(\epsilon) = \zeta(P(\epsilon), \rho) = \{\boldsymbol{x} \in R^8 : \boldsymbol{x}^T P(\epsilon)\boldsymbol{x} \le \rho\} \qquad \rho = \frac{1}{|\boldsymbol{b}^T P^{1/2}(\epsilon)|^2} \tag{27}$$

It is shown in the Appendix that if $\boldsymbol{x}_0 \in D(\epsilon)$, then $\boldsymbol{x}(t) \in D(\epsilon)$ and $|\boldsymbol{f}(\epsilon)\boldsymbol{x}(t)| \le 1 \quad \forall\ t > 0$. Hence, $D(\epsilon)$ is an invariant subset of the domain of attraction and is contained in the local linear region within the saturation bounds.

Theorem 2 establishes the existence of a saturation linear feedback law that guarantees the semiglobal stabilizability of the open-loop system (2). It is assumed that matrix $A_1$ is antistable, matrix $A_2$ is semistable, and $(A, \boldsymbol{b})$ is stabilizable. By definition, a linear system is semistable when it has poles located on the left-hand side or on the imaginary axis of the complex plane.

*Theorem 2* [9]: Let $\boldsymbol{f_0} = \boldsymbol{b}_1^T P1$. For any $\gamma_1 < 1$ and $\gamma_2 > 0$, there exist a $k > 0.5$ and an $\epsilon > 0$ such that $\Omega_1(\gamma_1) \times \Omega_2(\gamma_2)$ is contained in the domain of attraction of the equilibrium $\boldsymbol{x} = 0$ of the closed-loop system

$$\dot{\boldsymbol{x}} = A\boldsymbol{x} + \boldsymbol{b}u, \qquad u = \begin{cases} -\text{sat}(k\boldsymbol{f_0}\boldsymbol{x}_a), & \boldsymbol{x} \notin D(\epsilon) \\ -\text{sat}[\boldsymbol{f}(\epsilon)\boldsymbol{x}], & \boldsymbol{x} \in D(\epsilon) \end{cases} \tag{28}$$

The constructive proof of Theorem 2 is outlined next. It provides the design method and a description of the parameter variables that are required for control of the closed-loop system (28). The proof requires the construction of a set $D_1(\epsilon) \subset D(\epsilon)$, defined in Lemma 1. The positive definite matrix $P(\epsilon)$, referred to in Lemma 1, is the solution to the algebraic Riccati Eq. (25) with $P(\epsilon)$ of order $n \times n (A \in R^{n\times n})$:

$$P(\epsilon) = \begin{bmatrix} P_1(\epsilon) & P_2(\epsilon) \\ P_2^T(\epsilon) & P_3(\epsilon) \end{bmatrix}$$

where $P_1(\epsilon)$ is of order $2 \times 2$, $P_2(\epsilon)$ is of order $2 \times (n-2)$, and $P_3(\epsilon)$ is of order $(n-2) \times (n-2)$.

*Lemma 1*[9]: Denote

$$\tau_1(\epsilon) = \frac{1}{2\left|P_1^{1/2}(\epsilon)\right||\boldsymbol{b}^T P^{1/2}(\epsilon)|}$$

$$\tau_2(\epsilon) = \frac{-|P_2(\epsilon)| + \sqrt{[|P_2(\epsilon)|^2 + 3|P_1(\epsilon)||P_3(\epsilon)|]}}{|P_3(\epsilon)|}\tau_1(\epsilon)$$

Then

$$D_1(\epsilon) = \{\boldsymbol{x} \in R^n : |\boldsymbol{x}_a| \le \tau_1(\epsilon), |\boldsymbol{x}_s| \le \tau_2(\epsilon)\} \subset D(\epsilon) \tag{29}$$

Moreover,

$$\lim_{\epsilon\to 0}\tau_2(\epsilon) = \infty$$

and $\tau_1(\epsilon)$ increases with an upper bound as $\epsilon$ tends to zero.

*Proof of Theorem 2* [9]: It has been established for the closed-loop planar system

$$\dot{\boldsymbol{x}_a} = A_1\boldsymbol{x}_a - \boldsymbol{b}_1\ \text{sat}(k\boldsymbol{f_0}\boldsymbol{x}_a) \tag{30}$$

that the origin is the stable equilibrium for $k > 0.5$. Moreover, $\lim_{k\to\infty}\text{dist}[S(k), \mathcal{C}_1] = 0$, where $\mathcal{C}_1$ is the null-controllable region and $S(k)$ is the domain of attraction of $\boldsymbol{x}_a = \boldsymbol{0}$. Therefore, for $\gamma_1 < 1$ there exists $k > 0.5$ such that $\Omega_1(\gamma_1) = \{\gamma_1\boldsymbol{x}_a \in R^2 : \boldsymbol{x}_a \in \bar{\mathcal{C}}_1\} \subset S(k)$. For a given $\epsilon_0 > 0$ and an initial state $\boldsymbol{x}_{a\boldsymbol{0}} \in \Omega(\gamma_1)$, denote the trajectory of (30) as $\phi(t, \boldsymbol{x}_{a\boldsymbol{0}})$. Define

$$T(\boldsymbol{x}_{a\boldsymbol{0}}) = \min\{t \ge 0 : |\phi(t, \boldsymbol{x}_{a\boldsymbol{0}})| \le \tau_1(\epsilon_0)\}$$

Let

$$B_1 = \{\boldsymbol{x}_a \in R^2 : |\boldsymbol{x}_a| \le \tau_1(\epsilon_0)\}$$

$T(\boldsymbol{x}_{a\boldsymbol{0}})$ is the time that the trajectory $\phi(t, \boldsymbol{x}_{a\boldsymbol{0}})$ first enters the ball $B_1$.

Let

$$T_M = \max\{T(\boldsymbol{x}_{a\mathbf{0}}) : \boldsymbol{x}_{a\mathbf{0}} \in \partial\Omega_1(\gamma_1)\} \tag{31}$$

$$\gamma = \max_{t\in[0,T_M]} |e^{A_2 t}|\gamma_2 + \int_0^{T_m} |e^{A_2(T_M-\tau)}\boldsymbol{b}_2|\,\mathrm{d}\tau \tag{32}$$

By Lemma 1 there exists an $\epsilon < \epsilon_0$ such that $\tau_1(\epsilon) \geq \tau_1(\epsilon_0)$, $\tau_2(\epsilon) \geq \gamma$, and $D_1(\epsilon) \subset D(\epsilon)$ lies in the domain of attraction of the equilibrium $\boldsymbol{x} = \mathbf{0}$ of

$$\dot{\boldsymbol{x}} = A\boldsymbol{x} - \boldsymbol{b}\ \mathrm{sat}[\boldsymbol{f}(\epsilon)\boldsymbol{x}]$$

Consider an initial state $\boldsymbol{x}_0$ of Eq. (28), such that $\boldsymbol{x}_0 \in \Omega_1(\gamma_1) \times \Omega_2(\gamma_2)$. If $\boldsymbol{x}_0 \in D(\epsilon)$, then because $D(\epsilon)$ is an invariant set within the linear region of the domain of attraction, $\boldsymbol{x}(t)$ goes to the origin asymptotically. If $\boldsymbol{x}_0 \notin D(\epsilon)$, $\boldsymbol{x}(t)$ will enter $D(\epsilon)$ at some time $T \leq T_M$ because

$$\tau_1(\epsilon) \geq \tau_1(\epsilon_0) \Rightarrow B_1 \subset \{\boldsymbol{x}_a \in R^2 : |\boldsymbol{x}_a| \leq \tau_1(\epsilon)\}$$

under the control $u = -\mathrm{sat}(kf_0\boldsymbol{x}_a)$. If no saturation occurs (no switching to $\pm 1$), $\boldsymbol{x}_a(t)$ will hit the ball $B_1$ at time $T(\boldsymbol{x}_{a\mathbf{0}}) \leq T_M$ and $|\boldsymbol{x}_a[T(\boldsymbol{x}_{a\mathbf{0}})]| \leq \tau_1(\epsilon)$. By (32) $\gamma$ is a measure of the maximum magnitude of the state $\boldsymbol{x}_s(t)$ for $t \in [0 \quad T_M]$. At time $T(\boldsymbol{x}_{a\mathbf{0}})$

$$|\boldsymbol{x}_s[T(\boldsymbol{x}_{a\mathbf{0}})]| \leq \gamma \leq \tau_2(\epsilon)$$

which implies that

$$\boldsymbol{x}[T(\boldsymbol{x}_{a\mathbf{0}})] \in D_1(\epsilon)$$

From the preceding argument, it follows that if no saturation occurs, $\boldsymbol{x}(t)$ will be in $D_1(\epsilon)$ at $T(\boldsymbol{x}_{a\mathbf{0}})$. Because $D_1(\epsilon) \subset D(\epsilon)$, $\boldsymbol{x}(t)$ entered $D(\epsilon)$ at some time $T \leq T(\boldsymbol{x}_{a\mathbf{0}}) \leq T_M$. Therefore, we have shown for the case where no switching between $\pm 1$ occurs, that given an initial state $\boldsymbol{x}_0 \in \Omega_1(\gamma_1) \times \Omega_2(\gamma_2)$, $\boldsymbol{x}(t)$ enters the invariant set $D(\epsilon)$ at some time $T$ and tends asymptotically to the origin for time $t$ greater than $T$. In the case where switching is applied, once $\boldsymbol{x}(t)$ enters the invariant set $D(\epsilon)$ it will converge asymptotically to zero. □

## Algorithm for Analysis and Design

This section presents a summary in algorithm form of the theory for constructing a feedback control for the higher order linear BACT model. In general, it is assumed that the linear system is stabilizable and can be transformed into canonical model form consisting of a planar antistable subsystem, with one pair of complex eigenvalues, and a higher order stable subsystem.

1) Compute the boundary of the null-controllable region $\mathcal{C}_1$ of the antistable subsystem by solving Eq. (18) in terms of the time-reversed planar subsystem (16).

2) Construct sets $\Omega_1(\gamma_1)$ (23) and $\Omega_2(\gamma_2)$ (24) such that $\gamma_1 < 1$, $\gamma_2 > 0$, and $\Omega_1(\gamma_1)$ lies in the interior of $\mathcal{C}_1$.

3) For the antistable subsystem $A_1$ solve the ARE (8) for the unique positive definite matrix $P1$ and compute the feedback gain $\boldsymbol{f}_{\mathbf{0}} = \boldsymbol{b}^T P1$.

4) Determine the boundary of the domain of attraction $S(k)$ of the origin of the closed-loop system (5) by running the time-reversed system (20) for different values of $k$ such that the set $\Omega_1(\gamma_1)$ is a subset of the interior of $S(k)$. By applying Theorem 1, one may choose a $\hat{k} \geq k$ such that $S(\hat{k})$ is large enough to approximate the null-controllable region.

5) Construct an admissible state feedback law for the higher order BACT system (28) in the following manner: Choose an $\epsilon_0 > 0$ and solve for $P(\epsilon_0)$ the ARE (25). Compute $\tau_1(\epsilon_0)$ and $\tau_2(\epsilon_0)$ according to the formula of Lemma 1. Compute parameters $T_M$ (31) and $\gamma$ (32). By applying Lemma 1 and solving the ARE (25) find an $\epsilon < \epsilon_0$ such that $\tau_1(\epsilon) \geq \tau_1(\epsilon_0)$ and $\tau_2(\epsilon) \geq \gamma$. The feedback gain $\boldsymbol{f}(\epsilon) = \boldsymbol{b}^T P(\epsilon)$.

6) Construct $D(\epsilon)$ (27).

7) Select an initial condition within the set $\Omega_1(\gamma_1) \times \Omega_2(\gamma_2)$ (24).

8) Stabilize the higher order BACT model (2) using the feedback control law (28).

## Example

Consider open-loop plant #24 in canonical modal form (2):

$$A = \begin{bmatrix} A_1 & 0 \\ 0 & A_2 \end{bmatrix} = \begin{bmatrix} 1.5427 & 23.0449 & 0 & 0 & 0 & 0 & 0 & 0 \\ -23.0449 & 1.5427 & 0 & 0 & 0 & 0 & 0 & 0 \\ 0 & 0 & -4.1153 & 16.8314 & 0 & 0 & 0 & 0 \\ 0 & 0 & -16.8314 & -4.1153 & 0 & 0 & 0 & 0 \\ 0 & 0 & 0 & 0 & -14.8119 & 0 & 0 & 0 \\ 0 & 0 & 0 & 0 & 0 & -100 & 0 & 0 \\ 0 & 0 & 0 & 0 & 0 & 0 & -92.5700 & 136.9481 \\ 0 & 0 & 0 & 0 & 0 & 0 & -136.9481 & 92.5700 \end{bmatrix}$$

$$\boldsymbol{b} = \begin{bmatrix} -1823.519 \\ 239.443 \\ 409.586 \\ -771.637 \\ 1.549 \\ -1452878.399 \\ 1279858.07 \\ -3763625.593 \end{bmatrix}, \qquad \boldsymbol{x} = (\boldsymbol{x}_a, \boldsymbol{x}_s), \qquad \boldsymbol{x}_a = (x_1, x_2)$$

$$\boldsymbol{x}_s = (x_3, x_4, x_5, x_6, x_7, x_8)$$

Note that the antistable $2 \times 2$ submatrix $A_1$ contains one pair of complex eigenvalues and the stable $6 \times 6$ submatrix $A_2$ contains poles on the left-hand side of the complex plane. Moreover, $(A, \boldsymbol{b})$ is controllable and Theorem 2 directly applies. The desired set of initial conditions is $\Omega_1(\gamma_1) \times \Omega_2(\gamma_2)$ with $\gamma_1 = 0.9$ and $\gamma_2 = 10$. The parameter $\epsilon_0 = 1 \times 10^{-8}$. By computations of Lemma 1, $\tau_1(\epsilon_0) = 0.38953$.

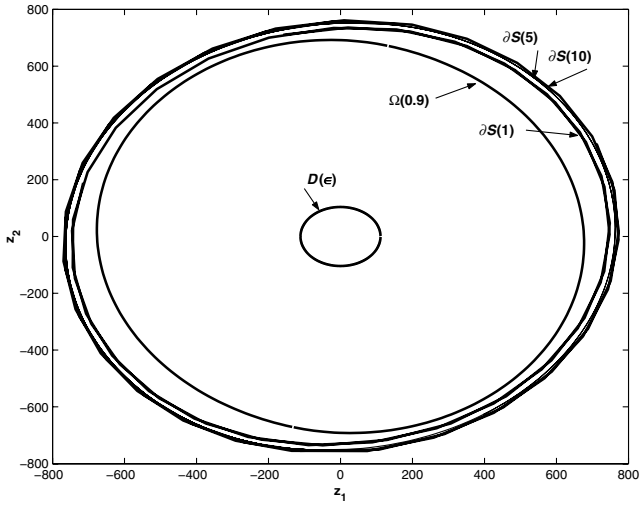


**Fig. 5 Boundaries of domains $S(k)$ and invariant set $D(\epsilon)$.**

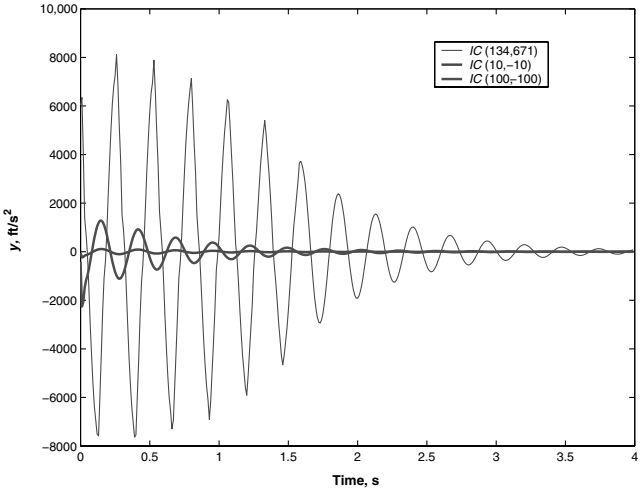


**Fig. 6 Output responses for plant #24.**

The following steps illustrate the method of parameter selection used in the control of plant #24 based upon Theorem 2 for the closed-loop system (28):

1) For $k = 1$, $\partial\Omega_1(0.9) \subset \partial S(1) \subset \partial\mathcal{C}_1$, where $S(1)$ is the domain of attraction of the origin of Eq. (5):

$$\dot{\boldsymbol{x}_a} = A_1\boldsymbol{x}_a - \boldsymbol{b}_1 \text{ sat}(\boldsymbol{f_0}\boldsymbol{x}_a)$$

$\boldsymbol{f_0} = \boldsymbol{b}_1^T P1 = [-0.0033 \quad 0.0007]$. $P1$ is the unique positive definite solution of the continuous time algebraic Riccati Eq. (8):

$$P1 = \begin{bmatrix} 0.000001793 & -0.000000116 \\ -0.000000116 & 0.000001872 \end{bmatrix}$$

2) $T_M = 6.37$ s follows from (31); $\gamma = 68,588$, from (32). $T(\boldsymbol{x}_{a\mathbf{0}})$ for each $\boldsymbol{x}_{a\mathbf{0}} \in \Omega_1(0.9)$ is obtained through simulation.

3) The parameter $\epsilon = 1 \times 10^{-11}$ is selected satisfying the criteria $\tau_1(\epsilon) > \tau_1(\epsilon_0)$ and $\tau_2(\epsilon) > \gamma$; $\tau_1(\epsilon) = 51.329$ and $\tau_2(\epsilon) = 113,220 > \gamma$; $D(\epsilon) = \zeta(P24(\epsilon), \rho)$ where $\rho = 0.02$.

Figure 5 demonstrates the set correspondences $D(\epsilon) \subset \Omega_1(0.9) \subset S(1) \subset S(5) \subset S(10)$. $D(\epsilon)$ is restricted to the antiplanar subsystem of plant #24. One can see from the figure that the boundaries of $S(5)$ and $S(10)$ are virtually identical.

Figures 6–8 demonstrate closed-loop system behavior and feedback control for "harsh" initial conditions located on or near the boundary of $\Omega_1(\gamma_1) \times \Omega_2(\gamma_2)$ with bounded control $|u(t)| \leq 1$. These initial conditions are meant to illustrate aspects of the theory at extremal conditions. The initial conditions of Figs. 9 and 10 are chosen to reflect the "benign" physical properties of the states of the original BACT model.

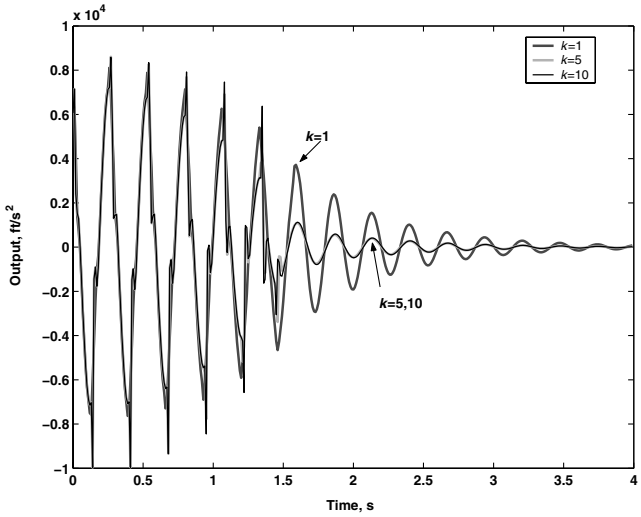


**Fig. 7 Output responses of closed-loop system for $k = 1, k = 5, k = 10$.**

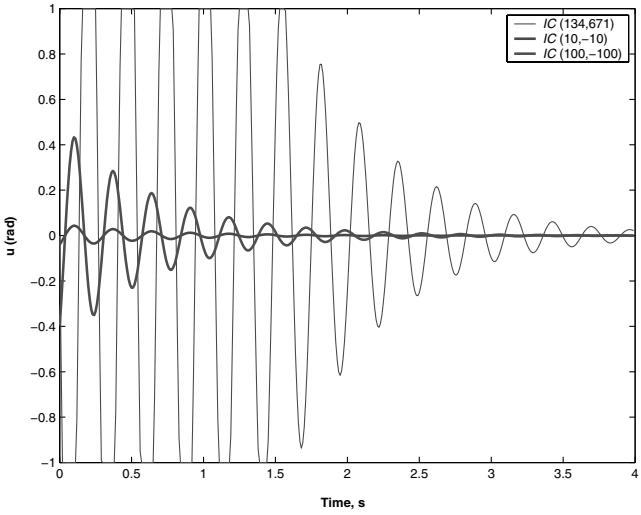


**Fig. 8 Control signal over three trajectories of closed-loop system.**

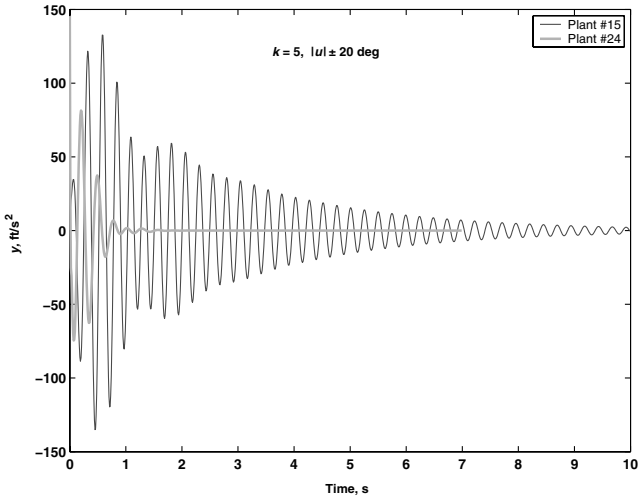


**Fig. 9 Accelerometer response of closed-loop system for plants #15 and #24.**

Figure 6 shows the closed-loop output responses for plant #24 (with density $\rho_{24} = 4 \times 10^{-3}$) starting from three different sets of initial conditions. The output response $y = \boldsymbol{C}\boldsymbol{x}$ (ft/s$^2$) where

$$C = [0.6262 \quad 9.2761 \quad -1.6490 \quad 6.7307 \quad -5.7457 \quad -0.5345 \quad 0.5940 \quad -0.0153]$$

Minimum entry times of the solution trajectory into the invariant set $D(\epsilon)$ vary with initial conditions in $\Omega_1(\gamma_1) \times \Omega_2(\gamma_2)$ and with $k$. For $k = 1$ and $\boldsymbol{x}_{a\mathbf{0}} = (x_1, x_2) = (134, 671) \in \partial\Omega_1(0.9)$ and $\boldsymbol{x}_{s\mathbf{0}} = (x_3, x_4, x_5, x_6, x_7, x_8) = (4, 4, 4, 4, 4, 4)(|\boldsymbol{x}_{s\mathbf{0}}| = 9.7 < \gamma_2 = 10)$, the minimum entry time is 2.28 s. For $\boldsymbol{x}_{a\mathbf{0}} = (100, -100) \in \Omega_1^{\circ}(0.9)$, the minimum entry time is 0.25 s. For $\boldsymbol{x}_{a\mathbf{0}} = (10, -10) \in \Omega_1^{\circ}(0.9)$, the minimum entry time is 0.01 s. For $\boldsymbol{x}_{a\mathbf{0}} = (134, 671) \in \partial\Omega_1(0.9)$ and $k = 2, 3, 5, 10, 100$, minimum entry times are 1.58, 1.53, 1.47, 1.46, and 1.47 s, respectively. The convergence of entry times at $k = 5, 10$, and 100 indicates that the boundary of $S(5)$ is a good approximation to the boundary of the null-controllable region.

Figure 7 shows the output responses of plant #24 for $k = 1$, $k = 5$, $k = 10$, for the initial condition of Fig. 6 on the boundary of $\Omega_1(0.9) \times \Omega_2(10)$. The responses for $k = 5$ and $k = 10$ overlap with slightly higher spikes for $k = 10$ during the period of oscillation before entering $D(\epsilon)$ between 1.46 and 1.47 s.

Figure 8 shows the behavior of the saturated control signal for the three trajectories of plant #24 shown in Fig. 6. The oscillations between $\pm 1$ occur for the trajectory with initial conditions $\boldsymbol{x}_{a\mathbf{0}} = (134, 671)$ and $\boldsymbol{x}_{s\mathbf{0}} = (4, 4, 4, 4, 4, 4)$ on the boundary of $\Omega_1(\gamma_1) \times \Omega_2(\gamma_2)$.

Figure 9 shows the response of the closed-loop system with gain factor $k = 5$ for the least unstable plant #15 with density $\rho_{15} = 2.2 \times 10^{-3}$ and the most unstable plant #24. For plant #15, the invariant set $\tilde{D}(\epsilon) = \zeta(P15(\epsilon), \rho)$, $\rho = 0.27$, where $P15(\epsilon)$ solves the ARE (25) for system matrix $A$ of plant #15. Clearly, the invariant set $D(\epsilon) = \zeta(P24(\epsilon), \rho)$, $\rho = 0.02$, is a strict and much smaller subset of $\tilde{D}(\epsilon)$. The control input $u$ is bounded by $\pm 20$ deg. The initial conditions for both plants are coordinate transformations of the following initial conditions of the BACT model:

$$\boldsymbol{x}_{\mathbf{0}}^{b} = [0.01(\mathrm{m}), 0.745(\mathrm{rad}), 0, 0.0175(\mathrm{rad/s}), 0, 0, 0, 0]^T$$

For this set of initial conditions no saturation occurs. Entrances into the invariant sets $\tilde{D}(\epsilon)$ and $D(\epsilon)$ take place during one simulation time step of 0.01 s.

Figure 10 shows the behavior of the feedback control $u$ during simulations of the trajectories shown in Fig. 9. The feedback control for plant #24 is bounded by $\pm 4.6$ deg($\pm 0.08$ rad). The feedback control for plant #15 is bounded by $\pm 0.46$ deg($\pm 0.008$ rad).

## Conclusions

NASA Langley Research Center's benchmark model was employed for demonstrating methods of construction of domains of attraction and the null-controllable region for the linear BACT system. Domains of attraction were constructed using time-reversed linear dynamics. A summary of the theory for constructing a saturation linear state feedback control law was presented for a system containing one pair of antistable complex eigenvalues. This paper presented simulations of the closed-loop systems for the least unstable and most unstable BACT models. Time-reversed dynamics allow one to choose a $k$ such that the domain of attraction is arbitrarily close to the null-controllable region. Simulations indicate that as $k$ is increased to allow for a close approximation to the null-controllable region, the performance, in terms of convergence times, also improves. In comparison with classical approaches and optimization methods that require extensive simulations and parameter adjustments, in controller design with bounded actuator feedback, this study demonstrates a theoretical approach that allows the designer to determine a priori the domain of attraction that will guarantee stabilization of the system.

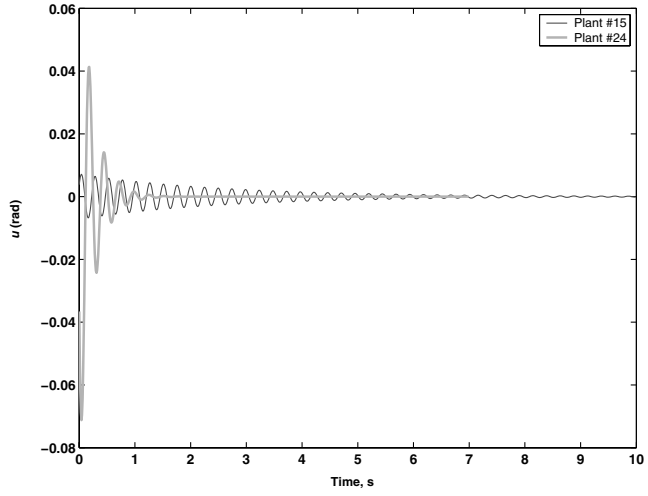


**Fig. 10 Control signal $u$ for BACT plant models #15 and #24.**

## Appendix: Properties of Set $D(\epsilon)$

*Claim*: The set $D(\epsilon)$ of Eq. (27) is a subset of $\{\boldsymbol{x}: |\boldsymbol{f}(\epsilon)\boldsymbol{x}| \leq 1\}$ where the gain $\boldsymbol{f}(\epsilon) = \boldsymbol{b}^T P(\epsilon)$, $P(\epsilon)$ the positive definite solution of the ARE (25). Moreover, $D(\epsilon)$ is an invariant set, i.e., for $\boldsymbol{x}_0 \in D(\epsilon)$, $\boldsymbol{x}(t)$ remains in $D(\epsilon)$ for all $t > 0$.

*Proof*: Repeating Eq. (27)

$$D(\epsilon) = \zeta(P(\epsilon), \rho) = \{\boldsymbol{x} \in R^8 : \boldsymbol{x}^T P(\epsilon)\boldsymbol{x} \leq \rho\}$$

$$\rho = \frac{1}{|\boldsymbol{b}^T P^{1/2}(\epsilon)|^2}$$

Simplifying and eliminating $\epsilon$ notation,

$$|\boldsymbol{b}^T P^{1/2}|^2 = (\boldsymbol{b}^T P^{1/2})(\boldsymbol{b}^T P^{1/2})^T = \boldsymbol{b}^T P^{1/2} P^{1/2} \boldsymbol{b} = \boldsymbol{b}^T P \boldsymbol{b}$$

Therefore,

$$\boldsymbol{x}^T P \boldsymbol{x} \leq \frac{1}{\boldsymbol{b}^T P \boldsymbol{b}} \Rightarrow \boldsymbol{x}^T P \boldsymbol{x} (\boldsymbol{b}^T P \boldsymbol{b}) \leq 1 \Rightarrow \boldsymbol{x}^T (\boldsymbol{b}^T P \boldsymbol{b}) P \boldsymbol{x} \leq 1$$

where the scalar $\boldsymbol{b}^T P \boldsymbol{b} > 0$ and $\boldsymbol{b}^T P \boldsymbol{b} P$ is positive definite.

Suppose $|\boldsymbol{f}(\epsilon)\boldsymbol{x}| = |\boldsymbol{b}^T P \boldsymbol{x}| \leq 1$ then $|\boldsymbol{b}^T P \boldsymbol{x}|^2 = \boldsymbol{x}^T P \boldsymbol{b} \boldsymbol{b}^T P \boldsymbol{x} \leq 1$. Symbolic calculations of MATLAB [19] show that $\boldsymbol{b}\boldsymbol{b}^T$ is positive semidefinite for any $n \times 1$ vector $\boldsymbol{b}$. It follows from this that the matrix $P\boldsymbol{b}\boldsymbol{b}^T P$ is positive semidefinite. It remains to show that if

$$\boldsymbol{x}^T \boldsymbol{b}^T P \boldsymbol{b} P \boldsymbol{x} \leq 1 \Rightarrow \boldsymbol{x}^T P \boldsymbol{b} \boldsymbol{b}^T P \boldsymbol{x} \leq 1 \tag{33}$$

Symbolic calculations of MATLAB show that for any $n \times n$ positive definite matrix P

$$\boldsymbol{b}^T P \boldsymbol{b} P - P \boldsymbol{b} \boldsymbol{b}^T P \geq 0$$

This implies that $\boldsymbol{x}^T (\boldsymbol{b}^T P \boldsymbol{b} P - P \boldsymbol{b} \boldsymbol{b}^T P) \boldsymbol{x} \geq 0$. Therefore, the implication (33) holds and $D(\epsilon) \subset \{\boldsymbol{x}: |\boldsymbol{f}(\epsilon)\boldsymbol{x}| \leq 1\}$ for $\boldsymbol{f}(\epsilon) = \boldsymbol{b}^T P$.

The invariance of the set $D(\epsilon)$ is shown as follows [20]. Consider the quadratic function $V(\boldsymbol{x}) = \boldsymbol{x}^T P(\epsilon)\boldsymbol{x}$, $\boldsymbol{x} \in D(\epsilon)$.

1) $V(\boldsymbol{x})$ is positive definite; and 2) The time derivative

$$\dot{V}(\boldsymbol{x}) = \dot{\boldsymbol{x}^T} P(\epsilon)\boldsymbol{x} + \boldsymbol{x}^T P \dot{\boldsymbol{x}} = -\boldsymbol{x}^T Q \boldsymbol{x} \leq 0$$

($Q$ a symmetric matrix), where the Lyapunov equation

$$[A - \boldsymbol{b}\boldsymbol{f}(\epsilon)]^T P(\epsilon) + P(\epsilon)[A - \boldsymbol{b}\boldsymbol{f}(\epsilon)] = -Q < 0$$

($Q$ positive definite). Conditions 1 and 2 imply that $V(\boldsymbol{x})$ is a Lyapunov function satisfying the conditions for local asymptotic stability of the origin for the system $\dot{x} = [A - \boldsymbol{b}\boldsymbol{f}(\epsilon)]\boldsymbol{x}$ and set invariance within $D(\epsilon)$.□

## Acknowledgments

The first author wishes to acknowledge Valery Glizer and Vladimir Turetsky for their expertise and suggestions regarding the assertion proved in the Appendix.

## References

[1] Waszak, M. R., "Robust Multivariable Flutter Suppression for Benchmark Active Control Technology Wind-Tunnel Model," *Journal of Guidance, Control, and Dynamics*, Vol. 24, No. 1, Jan.–Feb. 2001, pp. 147–153.

[2] Scott, R. C., Hoadley, Sh. T., Wieseman, C. D., and Durham, M. H., "Benchmark Active Controls Technology Model Aerodynamic Data," *Journal of Guidance, Control, and Dynamics*, Vol. 23, No 5, Sept.–Oct. 2000, pp. 914–921.

[3] Mukhopadhyay, V., "Transonic Flutter Suppression Control Law Design and Wind-Tunnel Test Results," *Journal of Guidance, Control, and Dynamics*, Vol. 23, No. 5, Sept.–Oct. 2000, pp. 930–937.

[4] Kelkar, A. G., and Joshi, S. M., "Passivity-Based Robust Control with Application to Benchmark Active Controls Technology Wing," *Journal of Guidance, Control, and Dynamics*, Vol. 23, No. 5, Sept.–Oct. 2000, pp. 938–947.

[5] Barker, J. R., and Balas, G. J., "Comparing Linear Parameter-Varying Gain-Scheduled Control Techniques for Active Flutter Suppression," *Journal of Guidance, Control, and Dynamics*, Vol. 23, No. 5, Sept.–Oct. 2000, pp. 948–955.

[6] Adin, Z., Ben-Asher, J., Cohen, K., Moulin, B., and Weller, T., "Flutter Suppression Using Linear Optimal and Fuzzy Logic Techniques," *Journal of Guidance, Control, and Dynamics*, Vol. 26, No 1, Engineering Notes, 2003, pp. 173–177.

[7] Applebaum, E., Ben-Asher, J., and Weller, T., "Fuzzy Gain Scheduling for Flutter Suppression in an Unmanned Aerial Vehicle," *Journal of Guidance, Control, and Dynamics*, Vol. 28, No 6, Nov.–Dec. 2005, pp. 1123–1130.

[8] Bhoir, N., and Singh, S. N., "Control of Unsteady Aeroelastic System via State-Dependent Riccati Equation Method," *Journal of Guidance, Control, and Dynamics*, Vol. 28, No. 1, Jan.–Feb. 2005, pp. 78–84.

[9] Hu, T., and Lin, Z., *Control Systems with Actuator Saturation, Analysis, and Design*, Birkhäuser Boston, Cambridge, MA, 2001, Chaps. 2, 4, 12.

[10] Alvarez, J., and Suarez, R., "Planar Linear Systems with Single Saturated Feedback," *Systems and Control Letters*, Vol. 20, No. 4, April 1993, pp. 319–326.

[11] Gutman, Per-Olof, and Per Hagander, "A New Design of Constrained Controllers for Linear Systems," *IEEE Transactions on Automatic Control*, Vol. AC-30, No. 1, Jan. 1985, pp. 22–23.

[12] Hu, T., and Lin, Z., "Output Regulation of Linear Systems with Bounded Continuous Feedback," *IEEE Transactions on Automatic Control*, Vol. 49, No. 11, Nov. 2004, pp. 1941–1953.

[13] Hu, T., Lin, Z., and Chen, B. M., "An Analysis and Design Method for Linear Systems Subject to Actuator Saturation and Disturbance," *Automatica: the Journal of IFAC, the International Federation of Automatic Control*, Vol. 38, No. 2, Feb. 2002, pp. 351–359.

[14] Macki, J., and Strauss, A., *Introduction to Optimal Control Theory*, Springer–Verlag, New York, 1982, Chap. 2.

[15] "ZAERO Theoretical Manual," Ver. 7, ZONA Technology, Scottsdale, AZ, Nov. 2003.

[16] Idan, M., Karpel, M., and Moulin, B., "Aeroservoelastic Interaction Between Aircraft Structural and Control Design Schemes," *Journal of Guidance, Control, and Dynamics*, Vol. 22, No. 4, July–Aug. 1999, pp. 513–519.

[17] Noble, B., and Daniel, J. W., *Applied Linear Algebra*, 3rd ed., Prentice Hall, Englewood Cliffs, NJ, 1988, Chap. 10.

[18] Anderson, B., and Moore, J., *Linear Optimal Control*, Prentice Hall, Englewood Cliffs, NJ, 1971, Sec. 5.3.

[19] "Symbolic Math Toolbox User's Guide," Ver. 3, Mathworks, Natick, MA, 1993–2005.

[20] Slotine, J-J, and Li, W., *Applied Nonlinear Control*, Prentice Hall, Englewood Cliffs, NJ, 1991, Chap. 3.